



Published in final edited form as:

Mol Cancer Ther. 2017 September ; 16(9): 1989–1998. doi:10.1158/1535-7163.MCT-17-0267.

Tyrosine Kinase Inhibitors Protect the Salivary Gland from Radiation Damage by Inhibiting Activation of Protein Kinase C- δ

Sten M. Wie¹, Elizabeth Wellberg², Sana D. Karam³, and Mary E. Reyland¹

¹Department of Craniofacial Biology, School of Dental Medicine, University of Colorado, Anschutz Medical Campus, Aurora, CO 80045, USA

²Department of Pathology, School of Medicine, University of Colorado, Anschutz Medical Campus, Aurora, CO 80045, USA

³Department of IR Oncology, School of Medicine, University of Colorado, Anschutz Medical Campus, Aurora, CO 80045, USA

Abstract

In patients undergoing irradiation therapy, injury to non-tumor tissues can result in debilitating, and sometimes permanent, side effects. We have defined Protein Kinase C-delta (PKC δ) as a regulator of DNA damage induced apoptosis and have shown that phosphorylation of PKC δ by c-Abl and c-Src activates its pro-apoptotic function. Here we have explored the use of tyrosine kinase inhibitors (TKIs) of c-Src and c-Abl to block activation of PKC δ for radioprotection of the salivary gland. Dasatinib, imatinib, and bosutinib all suppressed tyrosine phosphorylation of PKC δ and inhibited IR-induced apoptosis *in vitro*. To determine if TKIs can provide radioprotection of salivary gland function *in vivo*, mice were treated with TKIs and a single or fractionated doses of irradiation. Delivery of dasatinib or imatinib within 3 hours of a single or fractionated dose of irradiation resulted in >75% protection of salivary gland function at 60 days. Continuous dosing with dasatinib extended protection to at least 5 months and correlated with histological evidence of salivary gland acinar cell regeneration. Pretreatment with TKIs had no impact on clonogenic survival of HNSCC cells, and in mice harboring HNSCC cell derived xenografts, combining dasatinib or imatinib with fractionated irradiation did not enhance tumor growth. Our studies indicate that TKIs may be useful clinically to protect non-tumor tissue in HNC patients undergoing radiation therapy, without negatively impacting cancer treatment.

Keywords

Radioprotection; salivary gland; protein kinase C- δ ; tyrosine kinase inhibitor; head and neck cancer

Corresponding Author: Mary E. Reyland, Ph.D., Department of Craniofacial Biology, University of Colorado, Anschutz Medical Campus, Mail Stop 8120, P.O. Box 6511, Aurora, CO 80045, USA, Tel: 303-724-4572; Fax: 303-724-4580, Mary.Reyland@UCDenver.edu.

Conflict of Interest: The authors declare no potential conflict of interest.

Introduction

The majority of patients diagnosed with cancer will receive irradiation (IR) therapy either alone, or in combination with surgery or chemotherapy. Despite improvements in IR delivery, damage to healthy tissues, and the associated morbidities, can significantly impact quality of life. Furthermore, IR toxicity, especially in combination with chemotherapy, can limit the course of therapy, potentially impacting tumor eradication in some patients (1).

In the oral cavity, the oral mucosa and the salivary glands are highly sensitive to IR damage. Up to 40% of patients treated with IR for head and neck carcinoma (HNC) will develop moderate to severe xerostomia as a result of collateral damage to the salivary glands in the IR path (2). These patients typically experience a reduction in saliva production of >50% within a few weeks of commencing therapy (3). Salivary gland hypofunction, and the resultant xerostomia, is permanent and can have a significant impact on oral health and nutrition (2). Currently, the only therapeutic agent available to protect the salivary gland is the free radical scavenger, Amifostine, which is not widely used due to significant toxicity (4). Thus, there is a need for the development of new therapeutic strategies that will provide selective protection of these radiosensitive normal tissues without impacting tumor cell death.

We have previously shown that PKC δ is essential for apoptosis of salivary acinar cells *in vitro* and *in vivo* (5–10). PKC δ $-/-$ mice are protected from IR-induced damage to the salivary gland and thymus, and have a delay in mammary gland involution, a process driven by apoptosis (6,11). Likewise, salivary epithelial cells from PKC δ $-/-$ mice are resistant to multiple apoptotic stimuli including IR (6,12). Our studies have defined how PKC δ is activated in the context of apoptosis and have identified critical steps in this process that can be targeted therapeutically. Specifically, we have shown that nuclear targeting of PKC δ is necessary and sufficient for epithelial cell apoptosis, and that nuclear translocation requires phosphorylation of PKC δ at Y155 and Y64 by c-Abl and c-Src, respectively (5,10,13). Furthermore, we have shown that pretreatment of salivary acinar cells with the tyrosine kinase inhibitor (TKI) dasatinib, suppresses IR-induced apoptosis *in vivo*, and blocks phosphorylation of PKC δ at Y155 and Y64, and nuclear translocation of PKC δ *in vitro* (5).

As c-Abl and c-Src play fundamental roles in activating the pro-apoptotic function of PKC δ in IR treated tissues, we explored using TKIs with activity against c-Abl and/or c-Src for radioprotection of the salivary gland *in vivo*. Here we report that TKIs provide robust and durable protection of salivary gland function in a mouse head and neck IR model. Our studies suggest that TKIs may be useful clinically to protect non-tumor tissue in HNC patients undergoing IR without negatively impacting cancer therapy.

Materials and Methods

Cell Culture

The ParC5 cell line has been previously described (14). HNSCC cell lines (UMSCC19, Cal27 and FaDu) were cultured in DMEM/High glucose medium (Thermo Scientific, Logan, UT, USA, #SH30243.02) supplemented with 10% FBS (Sigma, St Louis, MO, USA,

#F2442). Cal27 and UMSCC19 cells were obtained in 2012 from Dr. Lynn Heasley (University of Colorado Anschutz Medical Campus) and FaDu cells were obtained in 2012 from Dr. Shi-Long Lu (University of Colorado Anschutz Medical Campus). Cell line profiling for authentication and mycoplasma testing was done at the DNA sequencing Core at University of Colorado Anschutz Medical Campus using the AmpFLSTR® Identifier® PCR Amplification Kit from Applied Biosystems. Cells used in these experiments were within 10 passages of testing. For some experiments cells were treated with dasatinib (5–50 nM) (University of Colorado Hospital Pharmacy), imatinib (0.1–10.0 µM) (University of Colorado Hospital Pharmacy), or bosutinib (0.1–1.0 µM) (Selleckchem, Houston, TX, USA, #SKI-606) 30 min prior to IR or treatment with H₂O₂ (Fisher Scientific, Waltham, MA #H325-500). Cells were irradiated using a Cesium-137 source.

In vivo Head and Neck IR

C57Bl/6 (#00664) and athymic nude (#002019) female mice were purchased from Jackson Laboratories (Bar Harbor, ME, USA). Animals were maintained at the University of Colorado, Anschutz Medical Campus, in accordance with Laboratory Animal Care guidelines and protocols and with the approval of the University of Colorado Denver Institutional Animal Use and Care Committee. For single dose IR, mice were anesthetized by intraperitoneal (i.p.) injection of 0.1mg/kg Avertin (Sigma #T4, 840-2), immobilized within a 50 mL conical tube, and a single dose of IR (10 or 15 Gy) was delivered to the head and neck using a Caesium-137 source. For fractionated IR, mice received 5 fractions of 6 Gy (tumor study) or 4 Gy (saliva production) on 5 consecutive days. Imatinib (50 mg/kg) and dasatinib (20 mg/kg) were given to mice via oral gavage at the indicated times. Control mice for imatinib and dasatinib were gavaged with water or citric acid buffer pH 2.1, respectively.

Saliva Collection

Saliva was collected immediately following i.p. injection of 0.1 mg/kg carbachol (Sigma, #C4382) in saline (0.9% NaCl). Whole saliva was collected for 3 mins from the lower cheek pouch using a suction device and expressed as mg (saliva)/g (mouse weight).

Analysis of Salivary Glands

For tissue analysis, salivary glands were formalin fixed, paraffin embedded, and sectioned at 5 µm. Tissue sections were stained with haematoxylin-eosin (H&E) and aquaporin 5 (AQP5) was detected by immunohistochemistry (Abcam, #ab78486). Stained slides were archived and analyzed using the Aperio Digital Pathology System and ImageScope software (Leica Biosystems). For AQP5, the number of positive stained pixels was quantified using the Positive Pixel algorithm in three representative sections, cut 50 µm apart, of both full submandibular salivary glands from two mice per treatment group, for a total of 6 measurements per group.

Lentivirus Transduction

ParC5 cells were transduced with lentivirus to transiently or stably express a non-specific “scrambled” shRNA (shScr) (Open Biosystems, Pittsburg, PA, USA #RHS4080) or rat PKCδ specific shRNAs (shδ1 and shδ3) (Open Biosystems, #RMM4331-98725640 and

RMM4331-99343143). For stable expression cells were maintained in media with 2 µg/mL puromycin. HNSCC cells were stably transduced with lentiviruses that express an shRNA targeting human PKCδ (shδ193 and shδ193) (Open biosystems, #TRC00010193, and #TRC00010203), or a non-targeting “scrambled” shRNA (shScr). Cells were maintained in media with 2 µg/mL puromycin.

Immunoblot Analysis

Immunoblotting was done as previously described (5). Antibodies to PKCδ (sc-937 and sc-213), PKCδ pY155 (sc-233770-R) and c-Abl (sc-23) were purchased from (Santa Cruz Biotechnology, Dallas, TX); anti- PKCδ pY64 was purchased from Assay Biotech, (#A8171, Sunnyvale, CA, USA). Antibodies against Src pY416 (#2110), Src family kinases (SFK) (#2108), Akt pS473 (#4060S), Akt (#9272S), ERK 44/42 pT202/pY204 (#4370S) and ERK (#4695S), and were purchased from (Cell Signaling, Beverley, MA). Anti-c-Abl pY412 was purchased from Novus Biological (#NB100-929665, Littleton, CO). The anti-actin antibody (ab49900) was purchased from (Abcam, Cambridge, England).

Caspase Assay

Active caspase-3/7 was detected using the Caspase-3/7 Cellular Activity Assay Kit PLUS (Biomol, Farmingdale, NY, USA, #BML-ALK7030001) according to the manufacturer’s instructions.

Clonogenic Survival

Cells expressing shScr or PKCδ specific shRNAs were plated at 500 (ParC5) or 100 (Cal27, FaDu, UMSSC19) cells per well in triplicate. Cells were treated with IR 24 hours after plating; for some experiments cells were treated with TKIs 30 minutes prior to IR. Media was replaced with media without TKIs 24 hours post IR. After 7–14 days, cells were fixed and stained with 0.5% crystal violet (Fisher Scientific, #C581-25) in –20°C methanol (Fisher Scientific, #A454-4) on ice, and colony number was quantified using Image J software. Data is graphed such that the number of colonies at 0 Gy represents the plating efficiency (PF=Average number of colonies/cells plated) and the surviving fraction represents the colony number for each dose of IR (SF=Average number of colonies/PE).

In vivo Tumor Analysis

FaDu cells (4×10^6) were suspended in 0.9% NaCl and injected subcutaneously into the right flank of nude mice. Mice were kept in a pathogen-free environment, and xenografts were measured by micro-caliper twice a week. When tumors reached 0.7 mm^3 (0.07 cm^3), mice were sorted by tumor size and randomized into the corresponding treatment groups. Dasatinib (20 mg/kg) and imatinib (50 mg/kg) were given following our pre/post regimen relative to each fraction of IR. Tumor volume was calculated using the equation ($\text{width}^2 \times \text{length}$)/2. Mice were sacrificed when tumors reached 2.0 cm^3 .

Statistical Analysis

Data were analyzed in Excel or in Graph Pad Prism 6. Shapiro-Wilk tests for normalcy were applied and if data were determined not to be normally distributed, non-parametric analyses

were performed. Otherwise, parametric statistical analysis was performed (t-tests, ANOVA). Graphical data are presented as mean \pm SEM unless otherwise noted.

Results

PKC δ is activated in response to IR and is required for IR-induced apoptosis in salivary gland acinar cells

We have previously shown that PKC δ ^{-/-} mice are resistant to IR-induced damage to the salivary gland and thymus and have a delay in mammary gland involution, a process driven by apoptosis (6,11). Our studies demonstrate that phosphorylation of PKC δ at Y64 and Y155 by c-Src and c-Abl, respectively, drives nuclear translocation, and is necessary and sufficient for the pro-apoptotic function of PKC δ (5,7,8). To determine if PKC δ is activated in response to IR, we examined phosphorylation of PKC δ at T505 in the activation loop of the kinase, and at Y64 and Y155 in the regulatory domain. Phosphorylation of PKC δ at T505 is seen within 1 hour after IR, while phosphorylation at Y64 and Y155 are detectable by 2 hours post IR and continue to increase until at least 6 hours (Figure 1A). To determine if PKC δ is required for IR-induced apoptosis, we assayed caspase activation in cells depleted of PKC δ with specific shRNAs (sh δ 1 and sh δ 3) or a scrambled shRNA (shScr). Expression of sh δ 3 reduced apoptosis by up to 50% relative to cells transfected with a scrambled shRNA control, and a similar trend was seen with sh δ 1 (Figure 1B).

TKIs block activation of PKC δ and suppress apoptosis

We have previously shown that both dasatinib and imatinib can block phosphorylation of PKC δ at Y64 and Y155, nuclear translocation of PKC δ and apoptosis in response to DNA damaging agents (5). Here we show that pretreatment of ParC5 cells with dasatinib, imatinib or bosutinib, all of which target c-Src and/or c-Abl, inhibits IR-induced apoptosis (Figures 1C–E). IR-induced apoptosis was reduced 40–60% by all TKIs, with bosutinib and imatinib being more potent than dasatinib. Likewise, activation of c-Abl and c-Src (SFK, Src family kinases) and phosphorylation of PKC δ at Y155 and Y64 were also suppressed by pretreatment with TKIs (Figure 1F–H). Interestingly, dasatinib and imatinib were slightly more potent inhibitors of Y155 phosphorylation than Y64 phosphorylation, consistent with their more potent inhibition of c-Abl than c-Src in ParC5 cells (Figure 1F and 1G).

TKIs protect salivary gland function in mice treated with head and neck IR

To explore radioprotection by TKIs *in vivo* we focused on dasatinib, a broad spectrum TKI, and imatinib, which preferentially inhibits c-Abl tyrosine kinase. The schematic in Figure 2A depicts the 3 dosing regimens used for the experiments in Figure 2. To determine if dasatinib (Figure 2B) or imatinib (Figure 2C) can protect salivary gland function, mice were dosed 1 hour before and 3 hours following IR delivery (“pre/post”) and production of whole saliva was assayed after 60 days. While whole saliva includes secretions from the 3 major salivary glands (submandibular, parotid and sublingual), the majority is produced by the submandibular glands (SMG). In mice that received IR plus vehicle, the saliva production was significantly reduced at 60 days post IR, reaching only 30% of the vehicle treated mice (Figure 2B). Dasatinib administration partially prevented the IR-mediated decrease in saliva production, and these mice produced 65% of the vehicle treated controls (Figure 2B).

Salivary gland function was protected to even a greater extent in mice treated with imatinib in conjunction with IR (Figure 2C); these mice retained >90% of their salivary function when treated with imatinib plus IR compared to IR alone.

We next asked if treatment with a single dose of dasatinib or imatinib prior to IR is sufficient for radioprotection (see Figure 2A “pre”), and if delivery of dasatinib or imatinib after IR affords radioprotection (see Figure 2A “post/post”). In the experiment shown in Figure 2D, saliva production after IR treatment was reduced by 70%. Remarkably, a single dose of dasatinib given prior to IR (pre), or 2 doses of dasatinib given post IR (post/post), offered similar protection as dosing mice pre/post IR (Figure 2D). All 3 treatment protocols with dasatinib resulted in nearly 100% protection of salivary gland function compared to vehicle only treated mice (Figure 2D). Similar results were seen in mice treated with imatinib (Figure 2E). Salivary gland function was > 80% of the vehicle control with pre/post or post/post-delivery of imatinib, while one dose prior to IR (pre) resulted in saliva production 63% of the vehicle control (Figure 2E).

In patients, decreased salivary gland function is seen in the first weeks after IR and is presumably due apoptosis of IR-damaged cells. In contrast, the inability to regenerate new salivary acinar cells presumably contributes to the permanent salivary gland hypofunction seen in many patients (2). Our studies demonstrate that dasatinib and imatinib can provide robust protection of salivary gland function for at least 60 days after delivery of IR. To address whether radioprotection persists beyond this time, we compared the effect of IR on saliva production in mice that received the pre/post treatment alone to mice that received the pre/post regimen and then continued to receive dasatinib twice a week for up to 5 months following a single dose of IR (see Figure 3A for scheme). As seen in Figure 3B, salivary function in mice that received IR alone was 50% of vehicle treated mice at 30 days, and decreased to 20% at 150 days. In comparison, in mice dosed only before and after IR (pre/post), saliva production at 30 and 60 days were 70% of vehicle treated mice, but declined thereafter (Figure 3B). Saliva production in this group were not significantly different from IR alone at 90, and 120 days. In contrast, mice that received continual dosing with dasatinib maintained a significantly higher level of salivary function out to 5 months. In this group, saliva production was 74% of vehicle treated controls at 90 days, 69% at 120 days, and 82% at 150 days after IR (Figure 3B).

Protection of salivary gland function in mice treated with dasatinib plus IR is suggestive of salivary gland tissue preservation, and/or increased gland regeneration. To ask if increased saliva production correlates with an increase in salivary acinar cell number, the experiment shown in Figure 3B was terminated after 150 days and the salivary glands were analyzed histologically. Staining with H&E revealed a decrease in salivary gland acinar cells in the SMGs of mice treated with IR alone, however this appeared to be largely reversed in mice that received continuous dosing with dasatinib (Figure 3C). To quantify the saliva-producing acinar cells, tissue sections from the entire salivary gland were stained by immunohistochemistry for expression of aquaporin 5 (AQP5), a specific acinar cell marker, and the relative expression of AQP5 across different treatment groups was quantified using Aperio Image Analysis software. In IR treated mice, the SMG acinar cell population was reduced by 60% compared to the SMGs of un-irradiated mice (Figure 3C–

D). This correlates with the 80% decrease in saliva production we reported in the IR alone treated mice (Figure 3B). Dasatinib treatment pre/post IR was not sufficient to prevent the decrease in acinar cells, consistent with our finding that in this treatment group saliva production was not different from the IR alone group at 150 days (Figure 3B). However, in IR treated mice continuously treated with dasatinib, the amount of AQP5 staining in the SMGs was 93% of that observed in vehicle treated mice, and consistent with protection of salivary gland function in this treatment group (Figure 3B).

Inhibition of PKC δ or treatment with TKIs does not promote survival of HNSCC cells

In order to be of benefit to patients, strategies to protect radiosensitive non-tumor tissues must not impact tumor eradication. To address this, we examined clonogenic survival and activation of cell survival pathways in Cal27, FaDu, and UMSCC19 HNSCC cell lines stably depleted of PKC δ , and in the context of TKI pre-treatment. Depletion of PKC δ had no impact on the clonogenic survival of any of the HNSCC cell lines analyzed (Figure 4A–C). Similarly, there was no change in clonogenic survival following IR of Cal27, FaDu or UMSCC19 cells treated with dasatinib, imatinib or bosutinib (Figure 4D–F). To confirm that TKI treatment does not affect pro-survival signaling, Cal27, FaDu and UMSCC19 cells were treated with dasatinib, IR or dasatinib plus IR. As seen in Figure 4G–I, while IR resulted in a modest increase in pAkt and/or pERK in Cal27 and FaDu cells, the addition of dasatinib had no effect, or reduced the level of activation.

TKIs do not enhance tumor growth when combined with fractionated IR

In patients IR is typically delivered in multiple fractions over 4–6 weeks. To assess the impact of TKIs on salivary gland function under similar conditions, we used a fractionated model where mice received 4 Gy IR to the head and neck on each of 5 consecutive days. Mice were dosed with imatinib before and after (pre/post) each fraction of IR. As shown in Figure 5A, in mice treated with IR alone, saliva production was reduced by 60% compared to the vehicle control group. However, in mice treated with IR plus imatinib, salivary gland function at 60 days after IR was not significantly different from the vehicle treatment alone, or imatinib only control groups, indicating that imatinib can provide protection of salivary gland function in a fractionated IR model.

We next asked if TKIs impact the growth of HNSCC tumor xenografts when delivered in combination with fractionated IR. FaDu cells were grown as flank xenograft tumors and mice were given 6 Gy of IR at the tumor site for 5 consecutive days. Before and after each IR treatment mice were dosed with either imatinib or dasatinib (pre/post dosing). Fractionated IR alone resulted in the attenuated growth of FaDu derived xenograft tumors (Figure 5B), and the addition of either dasatinib or imatinib had no effect on tumor growth. Interestingly, in mice treated with either dasatinib or imatinib alone there was a trend towards reduced tumor growth compared to their respective controls. Together, these data demonstrate that PKC δ inhibition is effective in protecting salivary gland function without sacrificing the cytotoxic effect of IR on HNC, and support evaluation of TKIs for radioprotection of the salivary gland in patients receiving IR for HNC.

Discussion

Nearly 60% of cancer patients will require IR at some point during their treatment, many of whom will suffer significant, and sometimes permanent, side effects due to IR damage to healthy non-tumor tissues in the radiation field (2). Acutely radiosensitive tissues that present significant clinical challenges include the hematopoietic system, gastrointestinal mucosa, and tissues in the oral cavity (1). Unfortunately, there is little to offer these patients, underscoring the need for new therapeutic strategies that provide selective protection of radiosensitive normal tissues without impacting tumor cell death. We have previously shown that PKC δ is required for IR-induced apoptosis in the salivary gland and that blocking activation of PKC δ with TKIs suppresses apoptosis (5). In this study we show that dasatinib and imatinib provide profound and durable protection of salivary gland function *in vivo* when delivered in conjunction with a single or fractionated doses of IR.

While most damage to non-tumor tissues in the oral cavity resolves in the months following IR, damage to the salivary gland, and the resulting xerostomia (“dry mouth syndrome”) can be permanent, particularly for those with locally advanced HNC (15,16). Considerable effort has been put into restoring the function of IR damaged glands by gene transfer of AQP5 into residual ductal cells, or regeneration of salivary gland tissue for re-implantation into IR damaged glands (17,18). Both of these approaches show remarkable promise for patients who suffer from severe loss of salivary gland function. However, the development of radioprotection agents that prevent IR-induced salivary gland damage is still a pressing need, and the availability of such agents would largely alleviate the need to repair or regenerate damage tissues. Attempts to protect salivary gland function have focused on use of free radical scavengers such as amifostine (4) to reduce cell injury, and growth factors such as FGF, IGF and KGF to stimulate gland regeneration (19–22). Our approach to reducing IR toxicity to the salivary gland is based on inhibiting the activation of PKC δ , a pro-apoptotic protein kinase required for DNA damage induced apoptosis *in vitro* and *in vivo* (23).

Tissue damage following IR is thought to be driven primarily by irreversible cell damage to replicating cells resulting in cell cycle arrest and apoptosis. While radiosensitive tissues typically have a high rate of cell turnover, the salivary glands are composed of highly differentiated cells that are thought to be primarily post-mitotic. In spite of this, widespread apoptosis is seen in the salivary glands of mice treated with 25 Gy of IR, especially within the first 24 hours (5). We have previously shown that activation of PKC δ by DNA damaging agents requires tyrosine phosphorylation by c-Abl and c-Src, and that TKIs of c-Abl and c-Src can block activation of PKC δ and DNA damage induced apoptosis *in vivo* (5). In our current studies we show that three different TKIs can suppress activation of PKC δ and apoptosis induced by IR *in vitro*, and demonstrate the efficacy of TKIs in radioprotection *in vivo*. A single dose of dasatinib or imatinib given prior to IR was sufficient to protect salivary gland function at least 60 days (Figure 2). Notably, delivery of TKIs at 3 and 6 hours post IR also protected salivary gland function, suggesting that TKIs may be useful in mitigating IR damage (Figures 2D and 2E). All TKIs tested are relatively broad spectrum, consistent with their ability to inhibit IR induced activation of both c-Abl and c-Src, and to suppress phosphorylation of both Y155 and Y64 on PKC δ (Figure 1C). Previous studies have also focused on inhibition of apoptosis as a strategy for radioprotection, particularly

through inhibition of p53 and p53 target genes (24,25). Notably, the pro-apoptotic function of PKC δ has been linked to the downstream activation of p53, and its transcriptional targets (p21 and PUMA), suggesting a mechanism through which suppression of PKC δ may reduce the apoptotic response (26,27). A report by Barckhausen *et al* also demonstrates that inhibition of apoptosis can promote DNA repair (28), consistent with a reported role for PKC δ in regulation of DNA repair (23).

Loss of salivary function following IR occurs more rapidly than can be accounted for by cell turnover alone, and models of “early” and “late” effects of IR have been proposed to explain this conundrum (29). Early effects of IR are seen within the first few weeks and likely result from direct damage to acinar cells resulting in impairment of secretory ability, and the subsequent loss of cells through apoptosis. In contrast, late effects presumably reflect an inability to regenerate new secretory cells due to loss of an epithelial progenitor population. Other “late” effects in the gland including inflammation and fibrosis may also impact the regenerative capacity of the gland. In our studies, salivary function is decreased by >50% at 30 days after IR and continues to decrease for at least 150 days, at which time only 20% of the functional capacity remains (Figure 3B). This is consistent with a decrease in AQP5 expression, which mark the secretory acinar cells, within the SMG (Figure 3D). While pre/post dosing with dasatinib protects function at 30 and 60 days, this effect is largely lost thereafter. Based on our studies demonstrating a critical role for PKC δ in apoptosis in the salivary gland *in vivo*, and studies in this manuscript which demonstrate that TKIs suppress IR-induced apoptosis (Figure 1B), we propose that suppression of acinar cell apoptosis contributes to the radioprotection observed in the first 30 to 60 days after IR by helping to maintain the secretory capacity of the gland. However, as salivary function continues to decline beyond 60 days, many of these cells must be eventually lost and not replaced.

In contrast to the pre/post-delivery of dasatinib, we show that continuous dosing of dasatinib in combination with IR results in sustained radioprotection and maintenance of SMG acinar cell number (Figure 3D). This suggests that TKIs may impact the regenerative capacity of the salivary gland. The simplest explanation is that TKIs protect a stem/progenitor cell pool that can be used to replace cells lost acutely through apoptosis. In this regard, reports using H³ and BrDu labeling demonstrate an acinar cell sub-population within the SMG capable of undergoing proliferation (30) and a number of groups have identified and cultured stem cell populations from rodent and human salivary glands (31). Notably, PKC δ has been shown to be important in the proliferation of stem cells from breast, pancreatic, prostate and melanoma tumors (32). More recently, Aure *et al.* described the ability of labeled acinar cells to undergo self-duplication within the parotid and submandibular glands (33). TKIs may also contribute to regeneration by suppressing IR-induced changes in the microenvironment. Studies in the skin, lung and kidneys show that IR can induce a chronic oxidative environment resulting in changes in expression of pro-inflammatory cytokines and a subsequent increase in apoptosis (34–37). Dasatinib is capable of interfering with the inflammatory response through inhibition of TNF- α , TGF-B and CXCR4 (38–40).

Our studies demonstrate the potential for TKIs to be used *in vivo* as a novel therapeutic approach for radioprotection of salivary gland function without accelerating tumor growth. In fact, our data suggests a trend toward suppression of tumor growth in mice treated with

dasatinib or imatinib alone (Figure 5B). This is consistent with clinical data where dasatinib given as a single agent failed to inhibit tumor growth, but also did not enhance tumor growth (41,42). The wide use of radiotherapy for various cancer patients suggests that TKIs may have broad implications in preventing harmful IR-related side effects. A recent report by Aigueperse *et al.* shows that the administration of dasatinib and the inhibition of c-Src protects against intestinal IR injury (43). Additionally, our results may have implications for side effects that result from chemotherapy, as a recent report by Pabla *et al.* demonstrates that PKC δ inhibition provides protection against cisplatin induced nephrotoxicity while simultaneously improving its cytotoxicity in tumor cells (44). These previous studies along with our current findings suggest that inhibition of PKC δ may be a promising therapeutic strategy for protection of non-tumor tissues in patients undergoing cancer therapy.

Acknowledgments

Financial support: NIH/NIDCR DE015648 and DE024309 to MER, and the University of Colorado Cancer Center support grant (NIH/NCI P30CA046934).

The authors appreciate the contribution to this research made by E. Erin Smith, Allison Quador, Jessica Arnold, and Andrea Osypuk of the University of Colorado Denver Research Pathology and Histology Shared Resource. This resource is supported in part by the Cancer Center Support Grant (P30CA046934). The authors would also like to thank Andrew Lewis, and Kelly Zaccane for their contributions to the animal work. Contents are the authors' sole responsibility.

References

1. Gudkov AV, Komarova EA. Radioprotection: smart games with death. *J Clin Invest American Society for Clinical Investigation*. 2010 Jul; 120(7):2270–3.
2. Vissink A, Mitchell JB, Baum BJ, Limesand KH, Jensen SB, Fox PC, et al. Clinical management of salivary gland hypofunction and xerostomia in head-and-neck cancer patients: successes and barriers. *Int J Radiat Oncol Biol Phys*. 2010 Nov 15; 78(4):983–91. [PubMed: 20970030]
3. Henson BS, Eisbruch A, D'Hondt E, Ship JA. Two-year longitudinal study of parotid salivary flow rates in head and neck cancer patients receiving unilateral neck parotid-sparing radiotherapy treatment. *Oral Oncol*. 1999 May; 35(3):234–41. [PubMed: 10621842]
4. Soref CM, Hacker TA, Fahl WE. A new orally active, aminothioli radioprotector-free of nausea and hypotension side effects at its highest radioprotective doses. *Int J Radiat Oncol Biol Phys*. 2012 Apr 1; 82(5):e701–7. [PubMed: 22330992]
5. Wie SM, Adwan TS, Degregori J, Anderson SM, Reyland ME. Inhibiting Tyrosine Phosphorylation of Protein Kinase C δ (PKC δ) Protects the Salivary Gland from Radiation Damage. *J Biol Chem*. 2014 Feb 25. jbc.M114.551366.
6. Humphries MJ, Limesand KH, Schneider JC, Nakayama KI, Anderson SM, Reyland ME. Suppression of apoptosis in the protein kinase Cdelta null mouse in vivo. *J Biol Chem*. 2006 Apr 7; 281(14):9728–37. [PubMed: 16452485]
7. DeVries-Seimon TA, Ohm AM, Humphries MJ, Reyland ME. Induction of apoptosis is driven by nuclear retention of protein kinase C delta. *J Biol Chem*. 2007 Aug 3; 282(31):22307–14. [PubMed: 17562707]
8. DeVries TA, Neville MC, Reyland ME. Nuclear import of PKCdelta is required for apoptosis: identification of a novel nuclear import sequence. *EMBO J*. 2002 Nov 15; 21(22):6050–60. [PubMed: 12426377]
9. Matassa AA, Carpenter L, Biden TJ, Humphries MJ, Reyland ME. PKCdelta is required for mitochondrial-dependent apoptosis in salivary epithelial cells. *J Biol Chem*. 2001 Aug 10; 276(32):29719–28. [PubMed: 11369761]

10. Adwan TS, Ohm AM, Jones DNM, Humphries MJ, Reyland ME. Regulated binding of importin- α to protein kinase C δ in response to apoptotic signals facilitates nuclear import. *J Biol Chem*. 2011 Oct 14; 286(41):35716–24. [PubMed: 21865164]
11. Allen-Petersen BL, Miller MR, Neville MC, Anderson SM, Nakayama KI, Reyland ME. Loss of protein kinase C delta alters mammary gland development and apoptosis. *Cell Death Dis*. 2010; 1(1):e17. [PubMed: 21364618]
12. Leitges M, Mayr M, Braun U, Mayr U, Li C, Pfister G, et al. Exacerbated vein graft arteriosclerosis in protein kinase Cdelta-null mice. *J Clin Invest*. 2001 Nov; 108(10):1505–12. [PubMed: 11714742]
13. Humphries MJ, Ohm AM, Schaack J, Adwan TS, Reyland ME. Tyrosine phosphorylation regulates nuclear translocation of PKCdelta. *Oncogene*. 2008 May 8; 27(21):3045–53. [PubMed: 18059334]
14. Anderson SM, Reyland ME, Hunter S, Deisher LM, Barzen KA, Quissell DO. Etoposide-induced activation of c-jun N-terminal kinase (JNK) correlates with drug-induced apoptosis in salivary gland acinar cells. *Cell Death Differ*. 1999 May; 6(5):454–62. [PubMed: 10381634]
15. Dijkema T, Raaijmakers CPJ, Haken Ten RK, Roesink JM, Braam PM, Houweling AC, et al. Parotid gland function after radiotherapy: the combined michigan and utrecht experience. *Int J Radiat Oncol Biol Phys*. 2010 Oct 1; 78(2):449–53. [PubMed: 20056347]
16. Dijkema T, Raaijmakers CPJ, Braam PM, Roesink JM, Monnikhof EM, Terhaard CHJ. Xerostomia: a day and night difference. *Radiother Oncol*. 2012 Aug; 104(2):219–23. [PubMed: 22809589]
17. Baum BJ, Alevizos I, Zheng C, Cotrim AP, Liu S, McCullagh L, et al. Early responses to adenoviral-mediated transfer of the aquaporin-1 cDNA for radiation-induced salivary hypofunction. *Proc Natl Acad Sci USA*. 2012 Nov 20; 109(47):19403–7. [PubMed: 23129637]
18. Ogawa M, Oshima M, Imamura A, Sekine Y, Ishida K, Yamashita K, et al. Functional salivary gland regeneration by transplantation of a bioengineered organ germ. *Nature Communications*. 2013 Oct 14:2498.
19. Guo L, Gao R, Xu J, Jin L, Cotrim AP, Yan X, et al. AdLTR2EF1 α -FGF2-mediated prevention of fractionated irradiation-induced salivary hypofunction in swine. *Gene Therapy*. 2014 Jul 17; 21(10):866–73. [PubMed: 25030610]
20. Lombaert IMA, Brunsting JF, Wierenga PK, Kampinga HH, de Haan G, Coppes RP. Keratinocyte growth factor prevents radiation damage to salivary glands by expansion of the stem/progenitor pool. *Stem Cells*. 2008 Oct; 26(10):2595–601. [PubMed: 18669914]
21. Limesand KH, Said S, Anderson SM. Suppression of Radiation-Induced Salivary Gland Dysfunction by IGF-1. *PLoS ONE*. 2009 Mar 24; 4(3):e4663. [PubMed: 19252741]
22. Choi J-S, Shin H-S, An H-Y, Kim Y-M, Lim J-Y. Radioprotective effects of Keratinocyte Growth Factor-1 against irradiation-induced salivary gland hypofunction. *Oncotarget*. 2017 Jan 10.
23. Reyland ME, Jones DNM. Multifunctional roles of PKC δ : Opportunities for targeted therapy in human disease. *Pharmacol Ther*. 2016 Sep; 165:1–13. [PubMed: 27179744]
24. Mustata G, Li M, Zevola N, Bakan A, Zhang L, Epperly M, et al. Development of small-molecule PUMA inhibitors for mitigating radiation-induced cell death. *Curr Top Med Chem*. 2011; 11(3): 281–90. [PubMed: 21320058]
25. Christophorou MA, Ringshausen I, Finch AJ, Swigart LB, Evan GI. The pathological response to DNA damage does not contribute to p53-mediated tumour suppression. *Nature*. 2006 Sep 14; 443(7108):214–7. [PubMed: 16957739]
26. Liu H, Lu Z-G, Miki Y, Yoshida K. Protein kinase C delta induces transcription of the TP53 tumor suppressor gene by controlling death-promoting factor Btf in the apoptotic response to DNA damage. *Mol Cell Biol*. 2007 Dec; 27(24):8480–91. [PubMed: 17938203]
27. Yoshida K, Liu H, Miki Y. Protein kinase C delta regulates Ser46 phosphorylation of p53 tumor suppressor in the apoptotic response to DNA damage. *J Biol Chem*. 2006 Mar 3; 281(9):5734–40. [PubMed: 16377624]
28. Barkhausen C, Roos WP, Naumann SC, Kaina B. Malignant melanoma cells acquire resistance to DNA interstrand cross-linking chemotherapeutics by p53-triggered upregulation of DDB2/XPC-mediated DNA repair. 2014 Apr 10; 33(15):1964–74.

29. Lombaert I, Movahednia MM, Adine C, Ferreira JN. Concise Review: Salivary Gland Regeneration: Therapeutic Approaches from Stem Cells to Tissue Organoids. *Stem Cells*. 2017 Jan; 35(1):97–105. [PubMed: 27406006]
30. Denny PC, Denny PA. Dynamics of parenchymal cell division, differentiation, and apoptosis in the young adult female mouse submandibular gland. *The Anatomical Record*. 1999 Mar 1; 254(3): 408–17. [PubMed: 10096673]
31. Pringle S, Van Os R, Coppes RP. Concise review: Adult salivary gland stem cells and a potential therapy for xerostomia. *Stem Cells*. 2013 Apr; 31(4):613–9. [PubMed: 23335219]
32. Chen Z, Forman LW, Williams RM, Faller DV. Protein kinase C- δ inactivation inhibits the proliferation and survival of cancer stem cells in culture and in vivo. *BMC Cancer BioMed Central*. 2014 Feb 14. 14(1):90.
33. Aure MH, Konieczny SF, Ovitt CE. Salivary gland homeostasis is maintained through acinar cell self-duplication. *Dev Cell*. 2015 Apr 20; 33(2):231–7. [PubMed: 25843887]
34. Robbins MEC, Zhao W. Chronic oxidative stress and radiation-induced late normal tissue injury: a review. *Int J Radiat Biol*. 2004 Apr; 80(4):251–9. [PubMed: 15204702]
35. François A, Milliat F, Guipaud O, Benderitter M. Inflammation and immunity in radiation damage to the gut mucosa. *Biomed Res Int*. 2013; 2013(22):123241–9. [PubMed: 23586015]
36. Kamata H, Honda S-I, Maeda S, Chang L, Hirata H, Karin M. Reactive oxygen species promote TNF α -induced death and sustained JNK activation by inhibiting MAP kinase phosphatases. *Cell*. 2005 Mar 11; 120(5):649–61. [PubMed: 15766528]
37. Siva, S., MacManus, M., Kron, T., Best, N., Smith, J., Lobachevsky, P., et al. A pattern of early radiation-induced inflammatory cytokine expression is associated with lung toxicity in patients with non-small cell lung cancer. In: LEE, YJ., editor. *PLoS ONE*. Vol. 9. 2014. p. e109560
38. Fraser CK, Lousberg EL, Kumar R, Hughes TP, Diener KR, Hayball JD. Dasatinib inhibits the secretion of TNF- α following TLR stimulation in vitro and in vivo. *Exp Hematol*. 2009 Dec; 37(12):1435–44. [PubMed: 19786067]
39. Bartscht T, Rosien B, Rades D, Kaufmann R, Biersack H, Lehnert H, et al. Dasatinib blocks transcriptional and promigratory responses to transforming growth factor- β in pancreatic adenocarcinoma cells through inhibition of Smad signalling: implications for in vivo mode of action. *Mol Cancer BioMed Central*. 2015 Nov 21. 14(1):199.
40. McCaig, AM., Cosimo, E., Leach, MT., Michie, AM. Dasatinib inhibits CXCR4 signaling in chronic lymphocytic leukaemia cells and impairs migration towards CXCL12. In: Gibson, SB., editor. *PLoS ONE*. Vol. 7. Public Library of Science; 2012. p. e48929
41. Lin Y-C, Wu M-H, Wei T-T, Chuang S-H, Chen K-F, Cheng A-L, et al. Degradation of epidermal growth factor receptor mediates dasatinib-induced apoptosis in head and neck squamous cell carcinoma cells. *Neoplasia*. 2012 Jun; 14(6):463–75. [PubMed: 22787428]
42. Brooks HD, Glisson BS, Bekele BN, Johnson FM, Ginsberg LE, El-Naggar A, et al. Phase 2 study of dasatinib in the treatment of head and neck squamous cell carcinoma. *Cancer*. 2011 May 15; 117(10):2112–9. [PubMed: 21523723]
43. Strup-Perrot C, Vozenin M-C, Monceau V, Pouzoulet F, Petit B, Holler V, et al. PrP(c) deficiency and dasatinib protect mouse intestines against radiation injury by inhibiting of c-Src. *Radiother Oncol*. 2016 Jul 9.
44. Pabla N, Dong G, Jiang M, Huang S, Kumar MV, Messing RO, et al. Inhibition of PKC δ reduces cisplatin-induced nephrotoxicity without blocking chemotherapeutic efficacy in mouse models of cancer. *J Clin Invest*. 2011 Jul; 121(7):2709–22. [PubMed: 21633170]

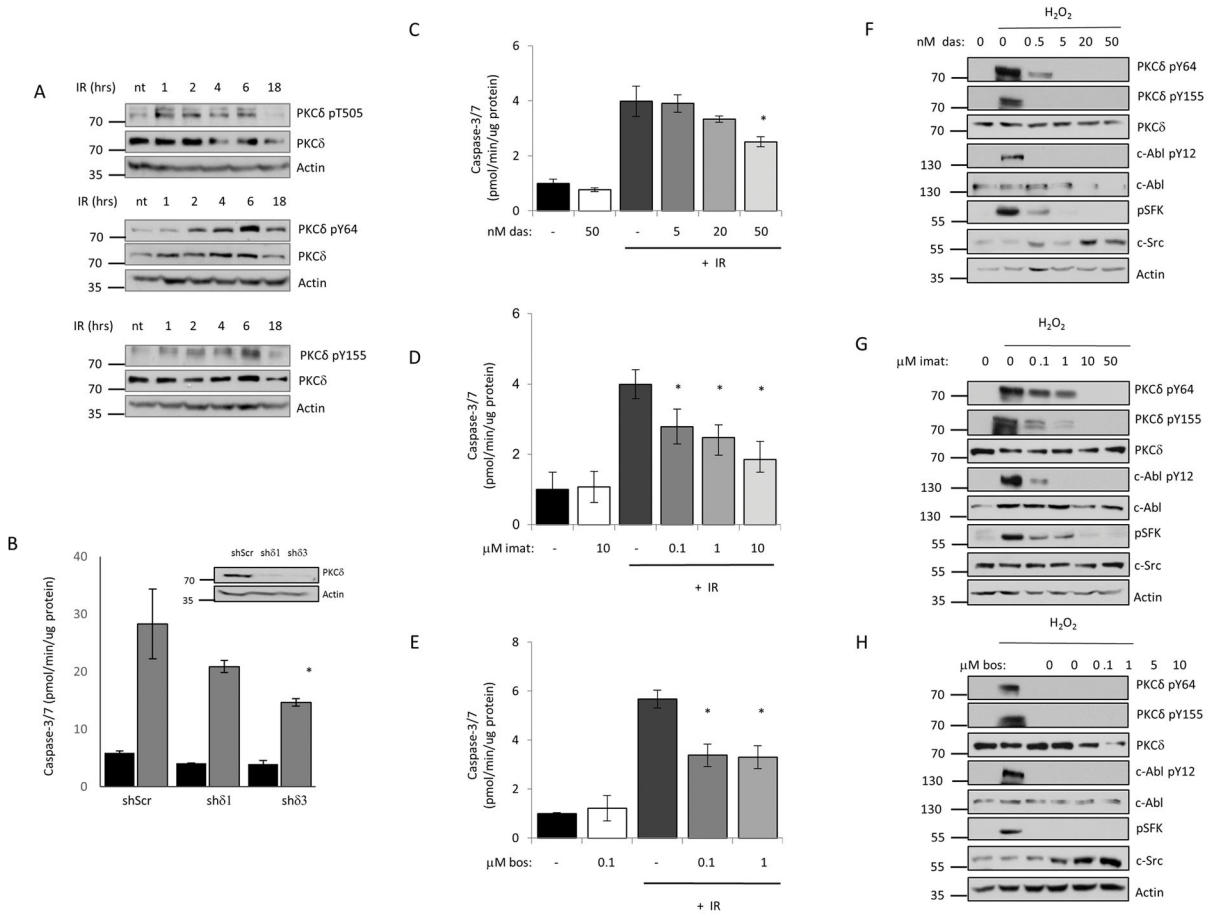


Figure 1. Tyrosine kinase inhibitors suppress tyrosine phosphorylation of PKCδ and IR induced apoptosis in salivary gland acinar cells

A, ParC5 cells were treated with 10 Gy IR and collected at the indicated time after IR. Whole cell lysates were resolved with SDS-PAGE and analyzed using phospho-specific antibodies that recognize PKCδ pY64, pY155 or pT505. Membranes were stripped and probed for total PKCδ and actin to determine loading. Each experiment was done a minimum of three times; representative immunoblots are shown. **B**, ParC5 cells were transiently infected with lentivirus expressing PKCδ specific shRNAs (shδ1 or shδ3) or a scrambled control shRNA (shScr), after 72 hours treated with IR (10Gy), and harvested after an additional 18 hr. Caspase-3/7 activity was assayed as described under “Methods”. Data shown is the average of triplicate samples from a representative experiment plus and minus the S.D. (error bars). The experiment was repeated three times, * = p<0.05 for caspase activity compared to cells expressing shScr. An immunoblot showing depletion of PKCδ is shown below. For panels **C–H**: ParC5 cells were treated with increasing concentrations of dasatinib (**C**, **F**), imatinib (**D**, **G**), or bosutinib (**E**, **H**) for 30 min, followed by treatment with 10 Gy IR (**C–E**), or the addition of 5 mM H₂O₂ for 30 min (**F–H**). **C–E**, Lysates were collected for caspase-3/7 activity analysis 18 hours after IR and was assayed as described under “Methods.” The data are the average of triplicate measurements from a representative experiment plus the S.D. (error bars). Each experiment was repeated three times. * = p<0.05 for caspase activity compared to cells treated with IR alone. **F–H**, Whole cell lysates were

collected 30 minutes after H₂O₂ treatment and analyzed by immunoblot for PKC δ pY64 and pY155. Inhibition of c-Src and c-Abl was determined by probing for their respective activation sites pY416 (c-Src) and pY412 (c-Abl). Blots were stripped and probed for total PKC δ , total SFK, total c-Abl and actin to determine total protein levels and loading efficiency. Each experiment was done a minimum of three times; representative immunoblots are shown.

Author Manuscript

Author Manuscript

Author Manuscript

Author Manuscript

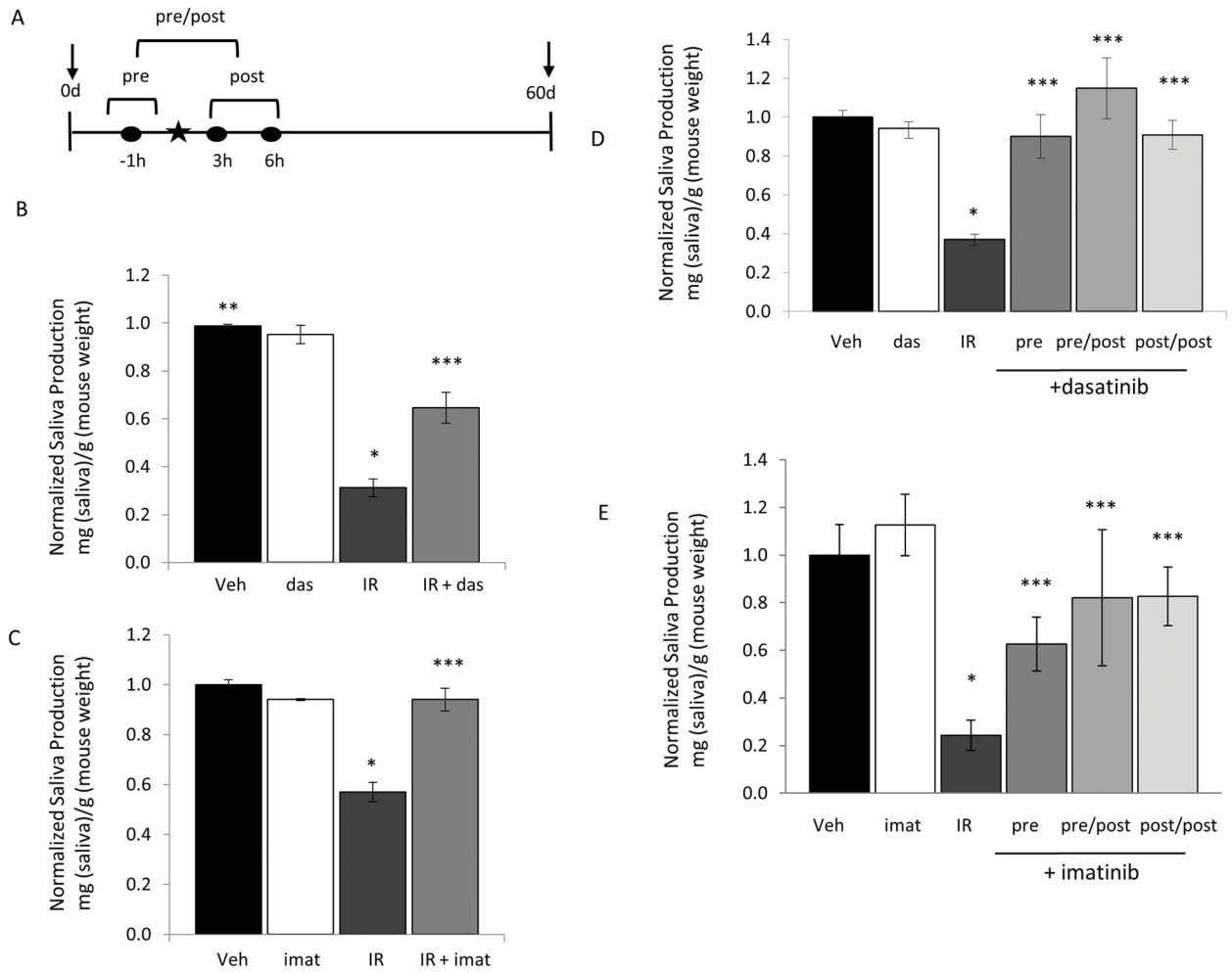


Figure 2. Treatment with TKIs protects against IR induced salivary gland damage

A, Experimental design of the experiments shown in panels **B–E**. The star indicates time of IR treatment. Three TKI dosing regimens were used, where times of delivery is indicated by the filled circles. Mice were treated with the specific TKI 1 hour prior to delivery of IR (pre), 1 hour prior and 3 hours post IR (pre/post), or 3 and 6 hours post (post/post). Saliva production was assayed prior to IR (day 0) and at 60 days after IR as described in Methods. **B–C**, Mice received vehicle alone (Veh), 15 Gy (B) or 10 Gy (C) IR plus vehicle, IR plus pre/post dosing of dasatinib (20mg/kg) (B) or imatinib (50 mg/kg) or TKI alone. **D–E**, Mice received vehicle, or IR plus dasatinib (D), imatinib (E) or vehicle using pre, pre/post, or post/post regimens. Saliva was collected i.p. as described in Methods. Salivary production (saliva weight/animal weight) for each cohort of mice was normalized against the saliva production for vehicle treated mice to generate the data shown. Data shown represents the average plus the S.E.M. (error bars) ($n > 3$). * = $p < 0.05$ saliva collected from mice which received IR alone compared to the vehicle treated mice. ** = $p < 0.001$ saliva collected from mice treated with vehicle compared to mice that received IR plus TKI treatment. *** = $p < 0.05$ saliva collected from mice treated with IR alone compared to mice that received TKI treatment with IR.

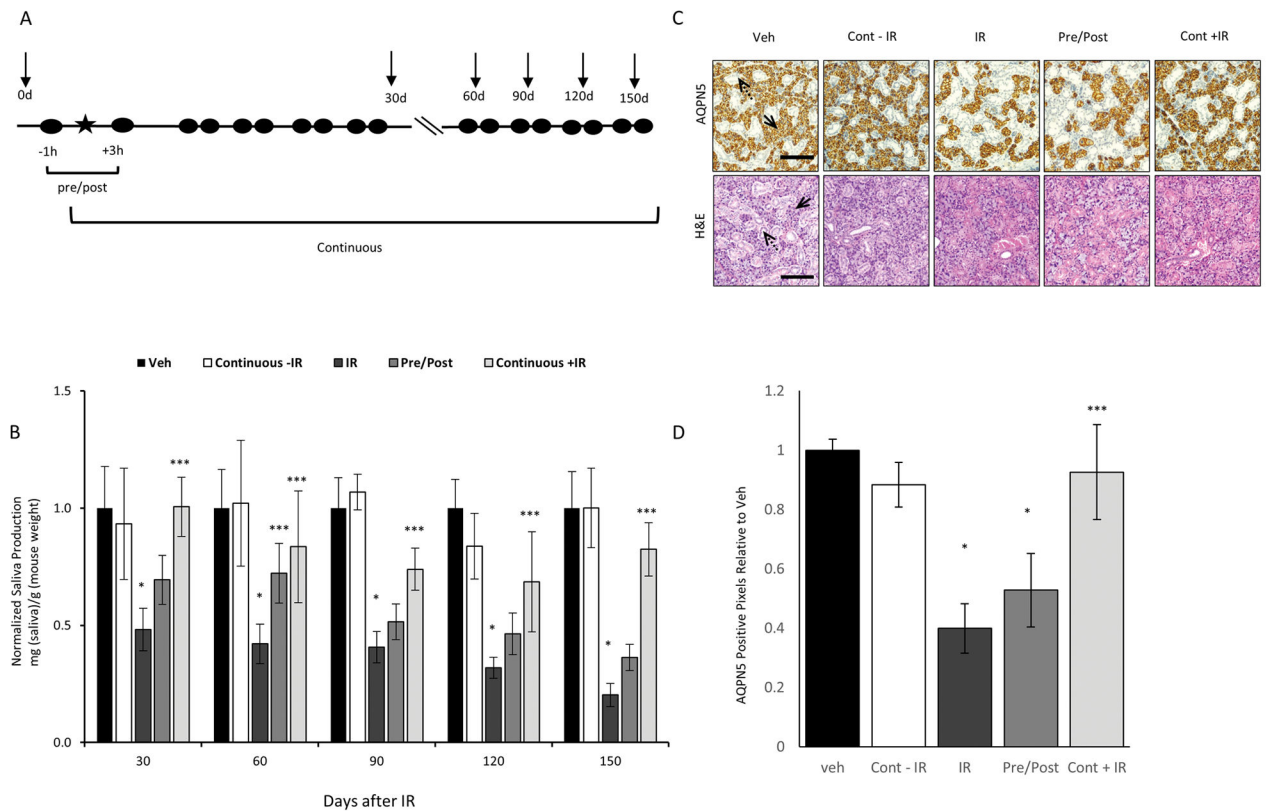


Figure 3. Continuous treatment with dasatinib results in durable protection of salivary gland function

A, Experimental design of pre/post and continuous dosing protocols. The star indicates time of IR treatment; while TKI delivery is indicated by the filled circles and arrows indicate time of saliva collection. Mice were dosed 1 hour prior and 3 hours post IR (pre/post), or pre/post plus twice a week for the duration of the experiment. Saliva production was assayed prior to IR (day 0) and at 30, 60, 90, 120 and 150 days after IR. **B**, Mice received vehicle alone, 15 Gy IR plus vehicle, or IR plus dasatinib as indicated. Saliva production (saliva weight/animal weight) for each cohort of mice was normalized against the production for vehicle treated mice to generate the data shown. Data represents the average plus the S.E.M. (error bars) ($n > 3$). * $= p < 0.01$ saliva collected from mice treated with IR compared to vehicle mice. *** $= p < 0.05$ saliva collected from mice treated with IR alone compared to mice that received TKI treatment with IR. **C–D**, Salivary glands from mice in each group ($n = 2$) were removed, formalin fixed and paraffin embedded. Immunohistochemistry for AQP5 and H&E staining was performed on salivary glands from each mouse. **C**, Shown are representative images (10X) of the SMG in each treatment group, scale = 100 μ m. Images were captured using an Olympus BX51 scope and Olympus DP72 camera with a 10 \times objective. Solid arrows indicate acinar cells while dashed arrows mark salivary gland ducts. **D**, Data shown represents the average number of AQP5 positive pixels plus the standard deviation (error bars) from 3 full representative sections of both SMG from 2 mice per treatment group. * $= p < 0.0001$ number of pixels in IR treated or pre/post treated mice

compared to vehicle treated mice. *** = $p < 0.0001$ number of pixels in IR treated mice compared to mice that received IR and continuous dasatinib treatment.

Author Manuscript

Author Manuscript

Author Manuscript

Author Manuscript

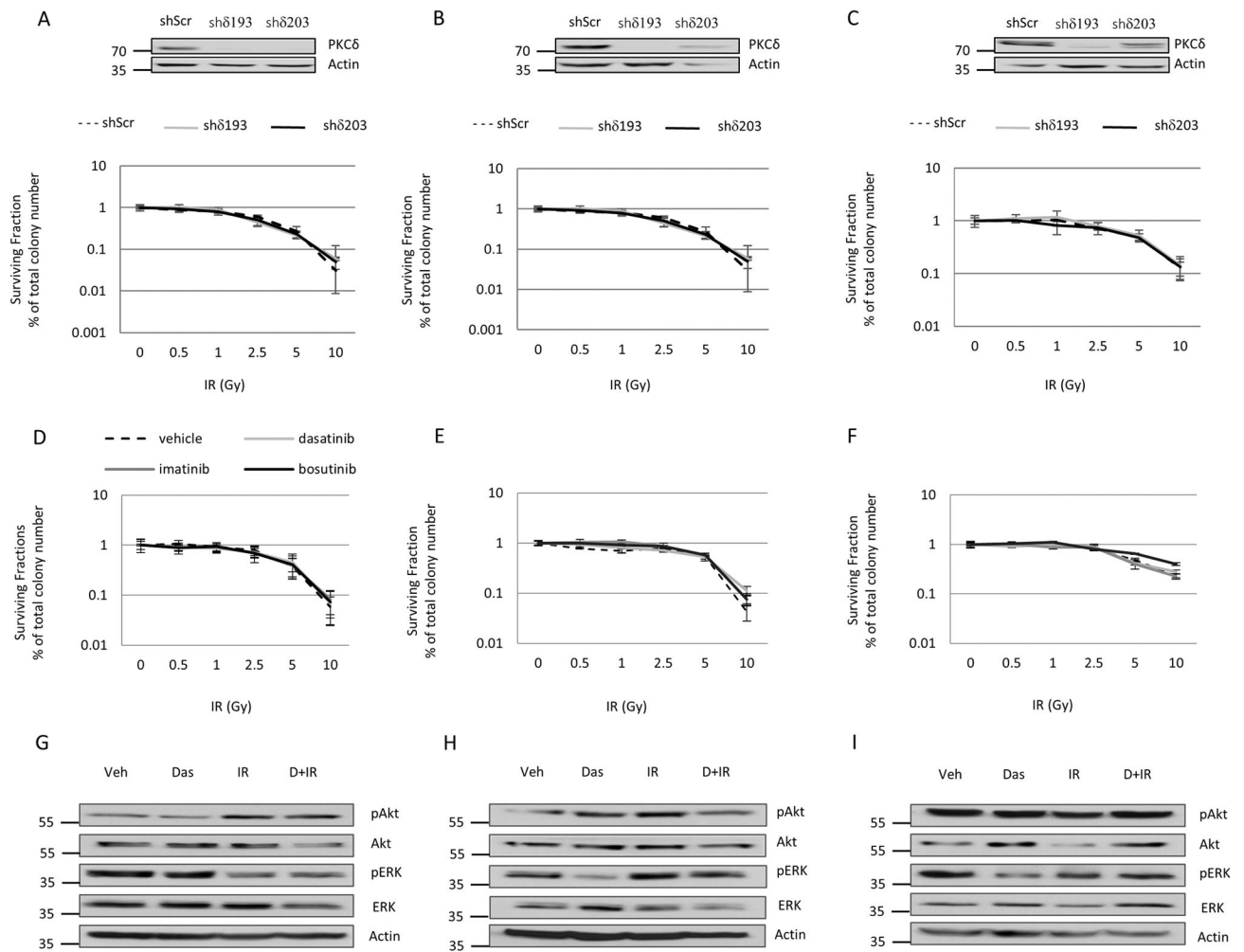


Figure 4. Depletion of PKC δ or treatment with TKIs does not enhance survival of HNSCC cells
A–C, Cal27 (A), FaDu (B), or UMSCC19 (C) HNSCC cells were stably transduced with lentivirus to express PKC δ specific shRNAs (sh δ 193 and sh δ 203) or a scrambled control (shScr). An immunoblot showing depletion of PKC δ is shown above. 24 hours after plating, cells were exposed to IR (0–10Gy). **D–F**, Cal27 (D), FaDu (E), and UMSCC19 (F) cells were plated, and 24 hours later were treated with DMSO (vehicle), dasatinib (50 nM), imatinib (10 μ M), or bosutinib (1 μ M) for 30 min prior to IR (0–10 Gy). **A–F**, Colonies were allowed to form over 10–14 days. The plating efficiency and surviving fractions from each condition was quantified using Image J as described in Methods. The data represents the average plating efficiency from three independent experiments plus the standard deviation (error bars). **G–I**, Cal27 (G), FaDu (H), and UMSCC19 (I) cells were treated with DMSO (Veh), 50 nM dasatinib alone (Das), or 10 Gy IR alone (IR), or given 50 nM dasatinib 30 min prior to 10 Gy IR (D + IR); cells were harvested 1 hour after IR. Whole cell lysates were analyzed for phospho-Akt and phospho-ERK, and stripped and probed for total Akt, total ERK, and actin. Shown are representative images from one experiment that was repeated three or more times.

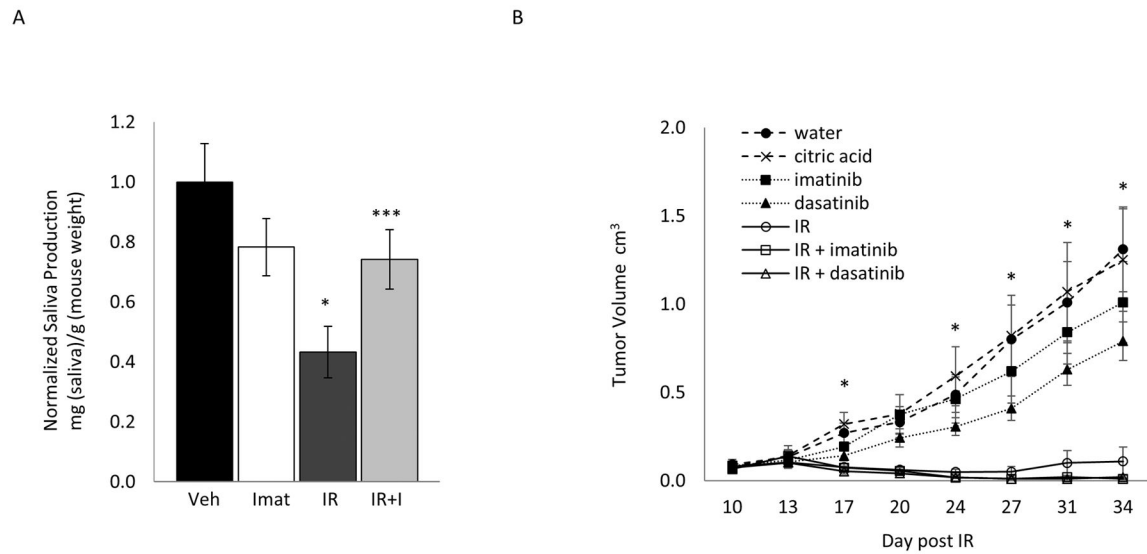


Figure 5. TKIs preserve salivary gland function without promoting tumor growth in a fractionated IR model

A, Mice were treated with imatinib (pre/post) relative to each fraction of IR (4 Gy) over 5 consecutive days. Saliva was collected prior to IR (day 0) and at 60 days after IR as described in Methods. Saliva production (saliva weight/animal weight) for each cohort of mice was normalized against the production for vehicle treated mice to generate the data shown. Data shown represents the average plus S.E.M. (error bars) ($n > 3$). * = $p < 0.01$ for saliva collected from radiated mice compared to vehicle treated mice. *** = $p < 0.05$ for saliva collected from mice treated with IR plus Imatinib compared to mice given IR alone. **B**, nude mice were injected with 4×10^6 log-phase FaDu cells. From day 10–14, mice received fractionated IR (5×6 Gy) with or without the pre/post treatment with either dasatinib or imatinib. Tumor volume was measured twice a week over the course of the experiment. On day 34 final measurements were collected. The data represents the average tumor size plus the S.E.M. (error bars) ($n > 7$). * = $p < 0.05$ for tumors in mice treated with dasatinib alone compared to citric acid (vehicle).